

Evidence from stellar rotation for early disc dispersal owing to close companions

S. Messina¹

INAF-Catania Astrophysical Observatory, via S.Sofia, 78 I-95123 Catania, Italy
e-mail: sergio.messina@inaf.it

ABSTRACT

Context. Young ($\lesssim 600$ Myr) low-mass stars ($M \lesssim 1 M_{\odot}$) of equal-mass exhibit a distribution of rotation periods. At the very early phases of stellar evolution, this distribution is set by the star-disc locking mechanism, which forces stars to rotate at the same rate of the disc inner edge. The primordial disc lifetime and, consequently, the duration of the disc-locking mechanism, can be significantly shortened by the presence of a close companion, making the rotation period distribution of close binaries different from that of either single stars or wide binaries.

Aims. We use new data to investigate and better constrain the range of ages, the components separation and the mass ratio dependence at which the rotation period distribution has been significantly affected by the disc dispersal that is enhanced by close companions.

Methods. We select a sample of close binaries in the Upper Scorpius association (age ~ 8 Myr) whose components have measured the separation and the rotation periods and compare their period distribution with that of coeval stars that are single stars.

Results. We find that components of close binaries have on average rotation periods shorter than single stars. More precisely, binaries with about equal-mass components ($0.9 \leq M_2/M_1 \leq 1.0$) have rotation periods on average by ~ 0.4 d shorter than single stars; binaries with smaller mass ratios ($0.8 < M_2/M_1 < 0.9$) have rotation periods on average by ~ 1.9 d the primary components, and by ~ 1.0 d the secondary components shorter than single stars. A comparison with the older 25-Myr β Pictoris association shows that, whereas in the latter all close binaries with projected separation $\rho \leq 80$ AU all rotate faster than single stars, in the Upper Scorpius that has happened for about 70% stars, yet.

Conclusions. We interpret the enhanced rotation in close binaries with respect to single stars as the consequence of an early disc dispersal induced by the presence of close companions. The enhanced rotation suggests that disc dispersal timescales are longest for single stars, then shorter for close binaries.

Key words. Stars: low-mass - Stars: rotation - Stars: binaries - Galaxy: open clusters and associations: individual: Upper Scorpius, - Stars: pre-main sequence - Stars: variables: T Tauri, Herbig Ae/Be

1. Introduction

Late-type stars ($M \lesssim 1 M_{\odot}$) with similar mass and age show a distribution of rotation periods. The width of such a distribution decreases as stars age, until a one-to-one correspondence between mass and rotation period is reached by an age of about 0.6 Gyr (e.g. Delorme et al. 2011). Such a distribution is though to arise from a distribution of the initial rotation periods, that is the rotation periods set during the disc-locking phase. Indeed, at the early stages of their life, most if not all stars are characterized by the presence of a primordial circumstellar disc that, while accreting mass and transferring angular momentum onto the star, leaves its imprinting, i.e. by fixing the value of the initial stellar rotation period. This happens by means of the disc-locking mechanism, which forces the star's outer layers to rotate for a few Myr at the rotation rate of the primordial disc inner edge (Shu et al., 1994). After the disc dispersal, such an imprinting still remains for long time, until the one-to-one correspondence is reached between mass and period and any memory of the initial rotation period gets lost.

Another parameter that effectively contributes to the

observed distribution of rotation periods among coeval equal-mass stars is the disc lifetime. The primordial disc lifetime is generally not longer than about 10 Myr (Ingleby et al. 2014; Ribas et al. 2014), but with exceptions (see, e.g. Frasca et al. 2015). However, such lifetime is variable and can be significantly shortened by different factors, the gravitational perturbation effects by a close companion being one of these. Once a star experiences either an early disc dispersion or inner disc truncation, its rotation rate starts spinning-up earlier than equal-mass disc-bearing stars, because of the radius contraction and angular momentum conservation, gaining a shorter rotation period in comparison.

Indeed, evidences have been so far accumulated showing that among coeval stars (i.e., members of the same association or cluster) disc-less members tend to rotate faster than disc-bearing members (Kraus et al. 2016, Cieza et al. 2009), as well as components of close binaries tend to have a smaller occurrence of discs and to exhibit shorter rotation periods (Stauffer et al. 2016, 2018; Rebull et al. 2018).

We intend to use the rotation period as a diagnostics to explore the effective existence of a disc dispersal enhancement, its dependence on the separation between

Send offprint requests to: Sergio Messina

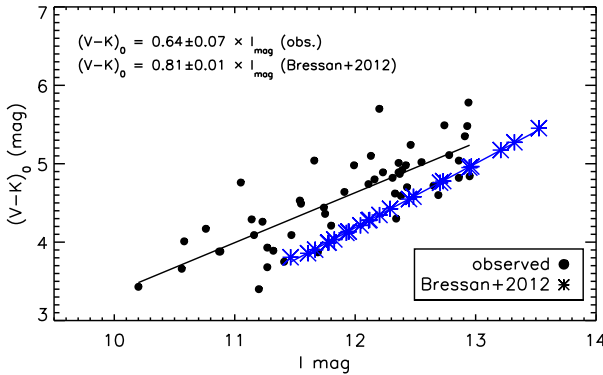


Fig. 1. Color de-reddened $(V-K)_0$ versus observed I mag for the sample observed by Tokovinin & Briceño (2018) (bullets). Blue asterisks represent the model I magnitudes, corrected for the distance modulus 5.8 mag (Wilkinson et al. 2018), and the model colors from Bressan et al. (2012). Solid lines are linear fits. We note that the model values are displaced on average by 0.75 mag from the magnitude of observed binary systems.

the binary components, on their mass ratio, and on the age. As already mentioned, the process of enhanced disc dispersal takes place by less than 10 Myr. Therefore, our investigation should better focus on clusters and association in this range of ages. Nonetheless, valuable information can be derived also from the analysis of older associations. Indeed, in the 25-Myr beta Pic Association, we found clear evidence for earlier disc dispersal induced by the presence of close companions. At that age, members of close binaries (projected separation < 80 AU) all rotate faster than their single counterparts (Messina et al., 2017).

Recently, two relevant investigations by Rebull et al. (2018) and Tokovinin & Briceño (2018) have made available accurate rotation period measurements and have newly imaged and spatially resolved a number of close binaries in the Upper Scorpius association at an age of ~ 8 Myr. This new information puts us in the position to push our investigation on the effects of binarity on disc dispersal, and then on rotation, back to a much younger age.

In this paper, we report the results of our analysis on the dependence of rotation on binarity at the age of about 8 Myr, more precisely among the low-mass candidate members of the young stellar association Upper Scorpius (USco). In Sect. 2 we describe the sample selection and the data. In Sect. 3 we present our analysis. In Sect. 4 we present discussion and interpretation. Conclusion are given in Sect. 5.

2. Sample selection

Rebull et al. (2018) have recently measured numerous rotation periods (~ 1000) in a sample of about 1300 candidate members of the young association USco. Interestingly, they report the finding of a sample of 239 candidate members showing multi-periodic light variations. They inferred periodicities by means of Lomb-Scargle periodogram analysis (Scargle, 1982) of the photometric time series collected during the Kepler K2 campaign.

Tokovinin & Briceño (2018) observed by means of spicule interferometry 129 among the brighter stars ($I < 13$ mag and $3 < (V-K)_0 < 6$ mag) of the multi-periodic sample of stars found by Rebull et al. (2018). They probed presence of companions in the separation range from $0.04''$ to $\sim 3''$, corresponding to separations from ~ 5 to ~ 400 AU. As result of their investigation, they spatially resolved 70 of them, giving additional support to the interpretation that multi-periodic stars are mostly binary stars. The sample selection criterion adopted by Tokovinin & Briceño (2018) advantaged the detection of binaries whose components have comparable flux; indeed most resolved components have magnitude difference $\Delta I < 1$ mag.

Compared to an isochrone of 8 Myr (Bressan et al., 2012), Tokovinin & Briceño (2018) found that their sample of resolved binaries is displaced on average by $\simeq +0.75$ mag above the isochrone, as expected for binary stars with nearly equal-mass components. They measured I_C magnitude, angular separation, magnitude difference between the resolved components, and derived the mass of the primary component (see their Table 1).

From the original Tokovinin sample of 70 resolved binaries, we selected a subsample of 49 targets in the color range $4 < (V-K)_0 < 6.5$ mag, in order to focus on only M-type stars.

The close binaries in our sample have mass ratio in the range $0.8 \leq M_2/M_1 \leq 1$, with only one binary with $M_2/M_1 = 0.65$. The mass ratio is derived using the mass of the primary component derived by Tokovinin & Briceño (2018) and the mass- I_{mag} relation from the 8-Myr isochrone (Bressan et al., 2012), transforming the observed magnitude difference ΔI into mass difference ΔM

$$\Delta M = M_1 - M_2 = \Delta I \times 0.197 \pm 0.014 \quad (1)$$

where 0.197 is the slope of the mass- I_{mag} relation in the M0–M6 spectral range.

3. Analysis

In the spectral range from M0 to about M6, we investigate if any difference exists between the period distribution of the 49 close binaries with known component's separation that we selected from the Tokovinin & Briceño (2018) sample and the period distribution of all single-star candidate members taken from Rebull et al. (2018).

Rebull et al. (2018) assumed that the periodicity P1 (which corresponds to the highest power peak in the Lomb-Scargle periodogram) is the rotation period of a single star or of the primary component of a multiple system. The second periodicity P2, when detected, (which corresponds to the second power peak in the Lomb-Scargle periodogram in order of decreasing power) is the rotation period of the secondary component of a multiple system. Therefore, P1 and P2 are the rotation periods of the components of the resolved close binaries in our analysis.

The dereddened $(V-K)_0$ colors provided by Rebull et al. (2018) for each photometric binary refers to the integrated system. Whereas, the primary and the secondary components have colors that are, respectively, bluer and redder than the integrated color. To derive the appropriate colors for both components we proceeded as follows. First we used the Bressan et al. (2012) models for the age of 8 Myr

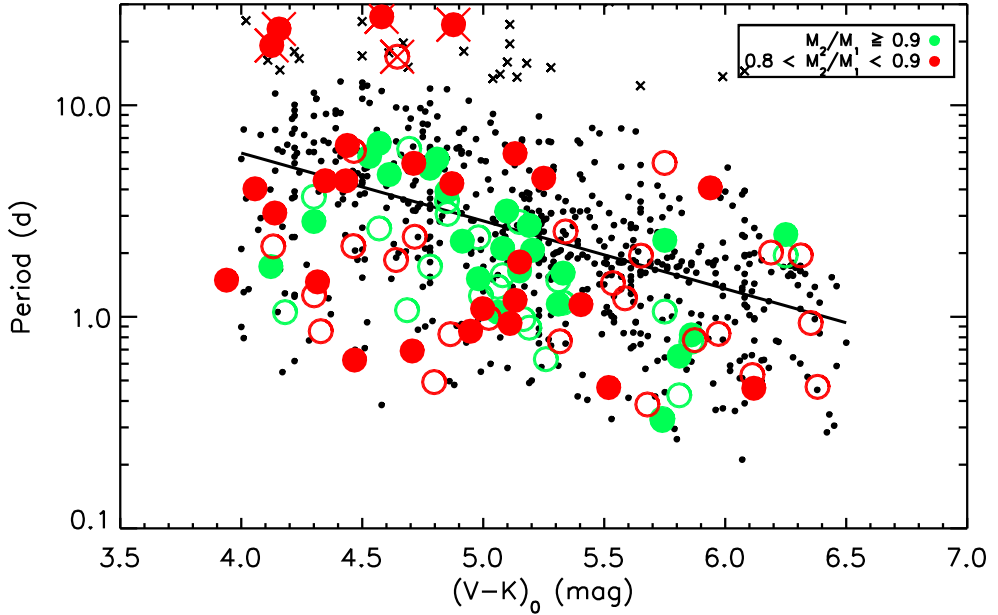


Fig. 2. Distribution of stellar rotation periods versus dereddened color for candidate members of the Upper Scorpius association from Rebull et al. (2018) in the M0–M6 spectral range. Small dots are the rotation periods of single stars as listed in Table 1 of Rebull et al. (2018). Filled and open bullets are periods P1 and P2 of components of close binaries. Green color denotes components of binary systems whose mass ratio is $M_2/M_1 \geq 0.9$, red color denotes components of binary systems whose mass ratio is $0.8 \leq M_2/M_1 < 0.9$. The solid line is a fit to the rotation periods of single stars (see Eq. (5)). Crossed symbols are outliers excluded from the fit computation and the following analysis.

to derive the color correction $\Delta(V - K)_{0P}$ for the primary component

$$\Delta(V - K)_{0P} = -2.5 \log \left(\frac{1 + \frac{F_{K2}}{F_{K1}}}{1 + \frac{F_{V2}}{F_{V1}}} \right) \quad (2)$$

where, F_{V1} and F_{V2} are the integrated fluxes in the V band, F_{K1} and F_{K2} in the K band, and P stands for primary component. We adopted for the primary components the colors $(V-K)_{0P} = (V-K)_0 + \Delta(V-K)_{0P}$.

Similarly, we computed the color correction $\Delta(V - K)_{0S}$ for the secondary component

$$\Delta(V - K)_{0S} = -2.5 \log \left(\frac{1 + \frac{F_{K1}}{F_{K2}}}{1 + \frac{F_{V1}}{F_{V2}}} \right) \quad (3)$$

We adopted for the secondary components the colors $(V-K)_{0S} = (V-K)_0 + \Delta(V-K)_{0S}$.

The color correction $\Delta(V - K)_{0S}$ for the secondary component (S), can be also computed by using the magnitude difference between the components ΔI measured by Tokovinin & Briceño (2018) and the linear regression coefficient ($a_1 = 0.64 \pm 0.07$) between the observed I magnitude provided by Tokovinin & Briceño (2018) and the reddening-corrected color $(V-K)_0$, as shown in Fig. 1.

$$\Delta(V - K)_{0S} = 0.64 \pm 0.07 \times \Delta I \quad (4)$$

We note that the model values of magnitude and color from Bressan et al. (2012) yield a larger value for the coefficient ($a_2 = 0.81 \pm 0.07$). We find that the use of a_1 and a_2 produce colors for the secondary components that are,

respectively 0.08 mag and 0.15 mag redder than those computed from Eq. (3). We found that the results of the following analysis remain substantially unchanged whichever is the method used to compute the colors of secondary components.

The relevant quantities taken from Tokovinin & Briceño (2018) and from Rebull et al. (2018) and the new ones computed in the present study for the selected 49 targets are listed in Table 1.

In Fig. 2 we plot the rotation period P versus $(V-K)_0$ color of all single-period candidate members using small dots and overplot the rotation period P1 (large filled bullets) and P2 (large open bullets) of the components of the 49 close binaries versus their colors, as computed according to Eqs. (2) and (3). Green color denotes components of binary systems whose mass ratio is $M_2/M_1 \geq 0.9$, red color denotes components of binary systems whose mass ratio is $0.8 \leq M_2/M_1 < 0.9$. The solid line is a fit to the rotation periods of single stars. All stars whose period residuals were larger than 3σ (i.e. $P - P_{fit} > 9.2$ d) were rejected (crosses in Fig. 2), and the new fit was computed

$$\log_{10} P = -0.304 \pm 0.020 \times (V - K)_0 + 1.94 \pm 0.10 \quad (5)$$

where P is the rotation period in days.

Before proceeding with our analysis, we must consider what follows. In unresolved close binaries, a fainter component whose flux ratio is, e.g., $F_2/F_1 \geq 0.6$, can exhibit activity-induced flux variability with amplitude $\geq 75\%$ of that exhibited by the primary component. This means that, depending on the specific properties of the activity patterns on the photosphere of both components, the variability arising from the secondary component may be dominant and

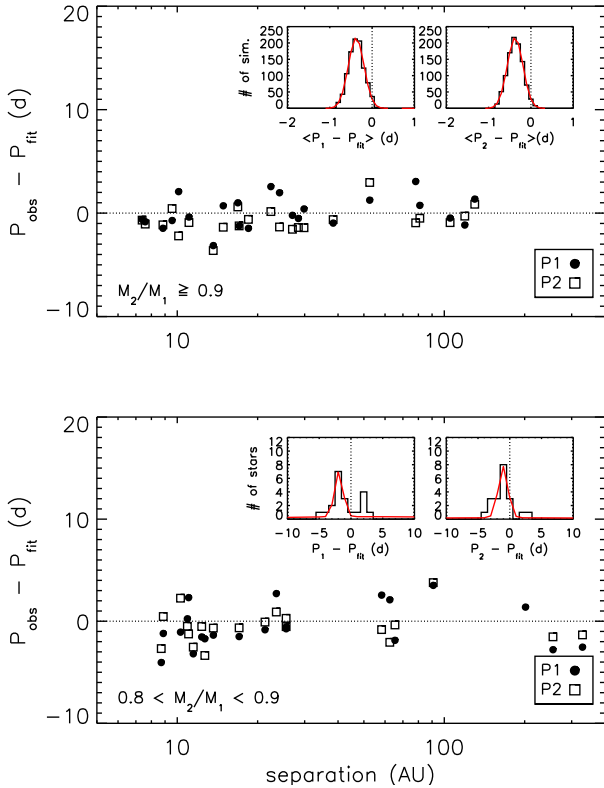


Fig. 3. Distribution of residuals of periods with respect to the fit (solid line in Fig. 2) for close binaries with about equal-mass components $M_2/M_1 \geq 0.9$ (top panel) and with non equal-mass components $0.8 \leq M_2/M_1 < 0.9$ (bottom panel). The top inner plots show the distribution of average $\langle P - P_{fit} \rangle$ residuals from Monte Carlo simulations (see text for explanation) with over plotted a Gaussian fit; the bottom inner plots show the distribution of the $P - P_{fit}$ residuals.

produce the most powerful peak in the periodogram. In this circumstance the primary period P_1 should be better attributed to the secondary component. Therefore, in our analysis we consider that rotation period P_1 and P_2 assigned by Rebull et al. (2018) to the primary and secondary components, respectively, in the case of close binaries with $F_2/F_1 \geq 0.6$, which corresponds to $\Delta I \leq 0.5$ mag ($\Delta M \leq 0.1 M_\odot$) may be exchanged.

We compute the difference between the primary periods P_1 and the fit (solid line in Fig. 2) and between the secondary period P_2 and the fit. This operation allows to remove the mass dependence of the rotation period. To explore any dependence of the rotation enhancement on the mass ratio between the components of a binary system, we consider two different mass ratio ranges: binaries whose components have about equal mass $M_2/M_1 \geq 0.9$ and binaries with smaller mass ratio $0.8 \leq M_2/M_1 < 0.9$. The rotation period residuals $P_{obs} - P_{fit}$ are plotted versus the component's projected separation in Fig. 3 (top panel for $M_2/M_1 \geq 0.9$ and bottom panel for $0.8 \leq M_2/M_1 < 0.9$). As previously done for the single stars, also components of binaries with period residuals larger than 3σ are not included in the following analysis (crossed symbols in Fig. 2). The circumstance that one binary's component has an outlying period does not necessarily imply that the binary is

not a member of the USco association. For example, the spot pattern on that component may have lead to measure the beat period instead of the rotation period. Therefore, we excluded from the analysis only the outlying component while keeping the rotation period of the other component.

In the case of close binaries with about equal-mass components, as explained above, we do not know to which components the P_1 and P_2 rotation periods refer. Then, we decided to make Monte Carlo simulations where the P_1 and P_2 periods of each binary are randomly permuted. We made 1000 of such simulations and for each we measured the average $\langle P_1 - P_{fit} \rangle$ and $\langle P_2 - P_{fit} \rangle$. The results of our simulations are plotted in the inner plots of the top panel of Fig. 3, where we plot in the form of histograms the distribution of the average $\langle P - P_{fit} \rangle$ for each of the 1000 simulations. We find that both periods P_1 and P_2 are shorter by $\simeq 0.4$ d, with respect to the average periods of single stars. We also find that the residuals P_1 -fit and P_2 -fit show some marginal evidence to be correlated to the projected separation between the binary components (top panel of Fig. 3). The Spearman's rank correlation analysis gives similar correlation coefficient $\rho = +0.29$ and significance p-value = 0.14 for P_1 -fit and P_2 -fit.

In the case of non equal-mass components (bottom panel of Fig. 3), we find that both periods P_1 and P_2 are shorter by $\simeq 1.9$ d and $\simeq 1$ d, respectively, with respect to the average period of single stars. The Spearman's rank correlation analysis gives a correlation coefficient $\rho = +0.17$ and significance p-value = 0.43 for P_1 -fit and $\rho = -0.11$ and significance p-value = 0.63 for P_2 -fit between residuals and projected separation.

To summarize, we find that candidate members of USco in close binaries (median separation ~ 21 AU in the analysed sample) rotate faster than their single counterparts; moreover, the lower-mass components of non-equal mass binaries tend to have the shortest rotation periods. We find some marginal evidence that the closer the equal-mass binary components, the faster their rotation period with respect to single stars.

Another property of our sample of close binaries, in addition to the average rotation period, is the period difference between the two components. We have seen that the rotation period is mass dependent; therefore, the period difference between the two components of the same system may arise on only their mass difference. For this reason, we first remove the mass dependence by computing the residuals with respect to a linear fit to the periods, then we compute the period differences and find that the average period difference between components of about equal-mass binaries ($M_2/M_1 \geq 0.9$) is $\langle \Delta P \rangle \simeq 0.8$ d (with a dispersion $\sigma = 1.6$ d) against $\langle \Delta P \rangle \simeq 0.2$ d (with a dispersion $\sigma = 1.9$ d) between the components of unequal-mass binaries ($0.8 \leq M_2/M_1 < 0.9$).

The last property that we take into consideration is the width of the period distribution (see Fig. 4). After removing the mass dependence, as already done before, we find that among binaries with about equal-mass components, primary and secondary components have residual distribution, respectively, smaller ($\sigma \simeq 0.7$ d) and larger ($\sigma \simeq 1.1$ d) than single stars ($\sigma \simeq 0.9$ d). Differently, among binaries with non equal-mass components, secondaries have similar residual distribution as single stars ($\sigma \simeq 0.9$ d), whereas primaries have a larger width of the residual distribution with a standard deviation $\sigma \simeq 1.1$ d.

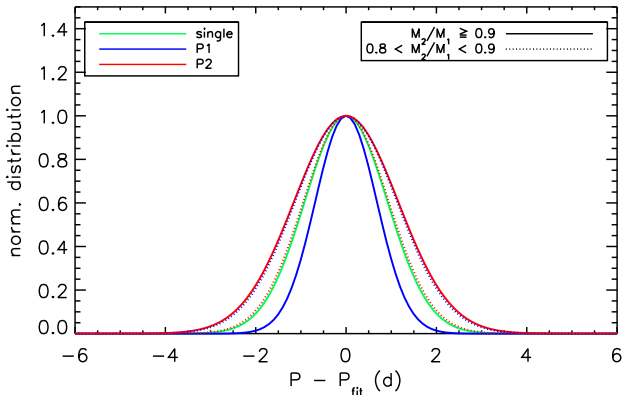


Fig. 4. Gaussian fits to the distribution of the residuals of the rotation periods: green line for single stars, blue line for primary components and red line for secondary components of binary systems. Note that the distributions for the P1 and P2 of binary components have been shifted to be centered on zero to make more easily readable the width difference.

Another important aspect concerns the fraction of discs. In the color range under analysis, about 28% of candidate members that are single (i.e. with only one periodicity measured) have strong evidence for a disc. If we consider the resolved close binaries in the same color range, we find that the fraction decreases to 14%.

4. Discussion

The disc lifetime is variable, but generally not longer than ~ 10 Myr (Ingleby et al. 2014, Ribas et al. 2014). Theories supported by observations predict that the disc lifetime can be significantly shortened by the presence of a companion (Meibom et al. 2007, Bouvier et al. 1993, Edwards et al. 1993, Ingleby et al. 2014, Rebull et al. 2004). Kraus et al. (2016) and Cieza et al. (2009) found that stars without IR excess tend to have companions at smaller separation than stars with excess indicating the presence of a disc. Both studies find that the depletion of primordial discs among binary systems with components closer than 40 AU is a factor 2 larger than in either single or wide binaries already at age as young as 1-2 Myr. Stauffer et al. (2016) report that photometric binaries among the Pleiades GKM-type stars tend to rotate faster than their counterpart single stars. Douglas et al. (2016) report that most, if not all, rapid rotators that deviate from the single-valued relation between mass and rotation already reached by the age of the Hyades (~ 0.6 Gyr), belong to multiple systems.

Recently, Messina et al. (2017) analyzing the rotation period distribution of the members of the 25-Myr β Pic Association found that single stars and components of multiple systems with projected separation larger than about 80 AU have similar distribution of rotation periods vs. the $V-K_s$ color. On the contrary, components of close visual binaries/triples with projected separation smaller than about 80 AU rotate preferentially faster than their equal-mass single counterparts. This circumstance suggests that when the components are sufficiently close, their primordial discs undergo an enhanced dispersal allowing the stars to start their spin up earlier than single stars.

The results by Messina et al. (2017) for the 25-Myr age can be compared to those we found at an age of 8 Myr for the USco association. In Fig.5, we plot the results of Messina et al. (2017), that is the relative residuals of the fit to the rotation period versus the projected separation (AU) as asterisks and overplot the same quantity but for the resolved binaries considered in this study as bullets. The use of residuals allows us to remove the mass dependence in the period distribution. We note that in the 5–80 AU range of projected separation about 70% of close binaries at the younger age of USco have period shorter (negative residuals) than their single counterparts, and about 30% still have periods comparable to those of the single stars. Differently, at the older age of the β Pic association, all close binaries have periods shorter than their single counterparts. This is a clear indication that the post-disc dispersal stellar rotation spin up is already set at ages younger than 8 Myr, and it has produced measurable effects on the majority of close binaries by an age of 8 Myr. The disc dispersal timescale in these close binaries must be different from binary to binary with a range of values so that there are close binaries (about 30% in this sample) where the dispersal takes place slowly making the rotation spin up not effective yet, as well as binaries, where the dispersal was quite sudden making the rotation spin up measurable.

We also note that the rotation period shortening for components of equal-mass binaries (~ 0.4 d for P1 and P2) is smaller than for non equal-mass binaries (~ 1.9 d for P1 and ~ 1.0 d for P2). This suggests that the timescale of their disc dispersal is dependent on the mass ratio between the binary components.

5. Conclusions

We have analyzed a sample of 49 close binaries which are candidate members of the Upper Scorpius association, whose components are in the M0–M6 spectral range, and have known rotation periods and projected separations ($\rho < 100$ AU). We found clear evidence that they rotate faster than their single counterparts. On average components of close binaries exhibit rotation periods shorter by an amount ranging from 0.4 d if they have about equal-mass to 1.9 d as in the case of the lower-mass components of lower mass-ratio binaries. The rotation spin up of close binaries with respect to single stars can be attributed, among different processes, to an early dispersion or truncation of the primordial circumstellar disc owing to gravitational effects by the close companion. Such a disc dispersal likely starts operating in the very first Myrs of stellar life, producing measurable effects at the age of 8 Myr.

In our hypothesis that the rotation period shortening with respect to single stars is a direct consequence of early disc dispersal, we infer that the timescale of disc dispersal is the longest in single stars or in wide-orbit ($\rho \gtrsim 100$ AU) components of multiple systems, then it is shorter in binaries with about equal-mass components and even shorter in binaries with non equal-mass components. Finally, we find that components of about equal-mass and of non equal-mass binaries generally have different rotation period dispersion widths, where primary components of equal-mass binaries exhibit a dispersion smaller than single stars, whereas

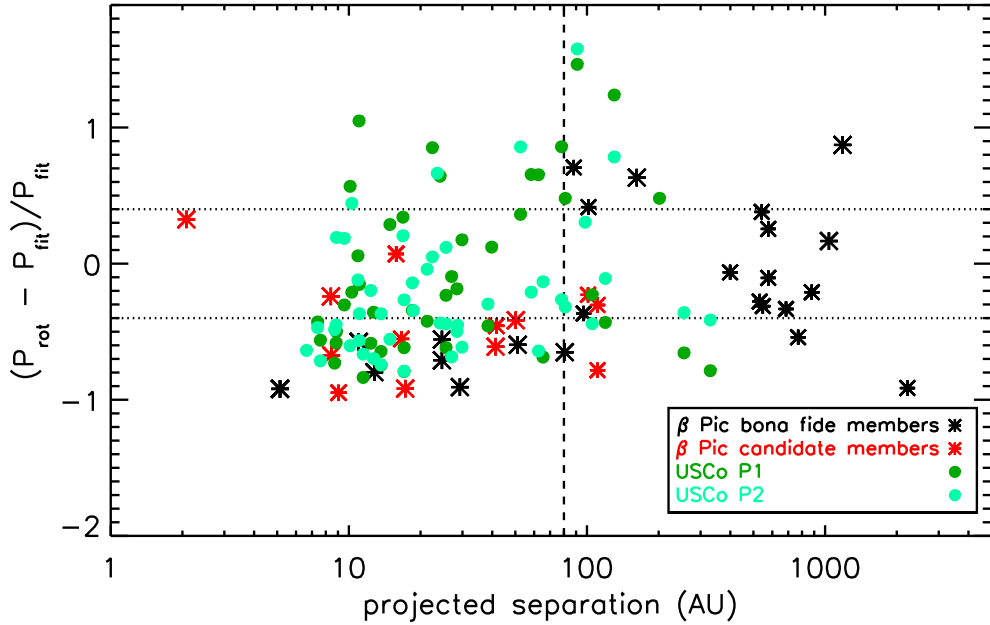


Fig. 5. Comparison between the distribution of relative period residuals versus projected separation for the members of the β Pic association (see also Fig. 7 of Messina et al. 2017) and the close binaries candidate members of Upper Scorpius. Horizontal dotted lines represent the width ($\pm 3\sigma$) of the period distribution of the β Pic single members. In the β Pic association, close binaries with component separation < 80 AU (vertical dashed line) mostly rotate faster than single stars.

secondaries and components of non equal-mass binaries all exhibit dispersion comparable to or larger than single stars.

Tokovinin, A. & Briceño, C. 2018, AJ, 156, 138
 Wilkinson, S., Merín, B., & Riviere-Marichalar, P. 2018, A&A, 618, A12

Acknowledgements. Research on stellar activity at INAF- Catania Astrophysical Observatory is supported by MIUR (Ministero dell’Istruzione, dell’Università e della Ricerca). This research has made use of the Simbad database, operated at CDS (Strasbourg, France). We are grateful to the Referee who allowed us to significantly improve the quality of this paper.

References

Bouvier, J., Cabrit, S., Fernandez, M., Martin, E. L., & Matthews, J. M. 1993, A&A, 272, 176
 Bressan, A., Marigo, P., Girardi, L., et al. 2012, MNRAS, 427, 127
 Cieza, L. A., Padgett, D. L., Allen, L. E., et al. 2009, ApJ, 696, L84
 Delorme, P., Collier Cameron, A., Hebb, L., et al. 2011, MNRAS, 413, 2218
 Douglas, S. T., Agüeros, M. A., Covey, K. R., et al. 2016, ApJ, 822, 47
 Edwards, S., Strom, S. E., Hartigan, P., et al. 1993, AJ, 106, 372
 Frasca, A., Biazzo, K., Lanzafame, A. C., et al. 2015, A&A, 575, A4
 Ingleby, L., Calvet, N., Hernández, J., et al. 2014, ApJ, 790, 47
 Kraus, A. L., Ireland, M. J., Huber, D., Mann, A. W., & Dupuy, T. J. 2016, AJ, 152, 8
 Meibom, S., Mathieu, R. D., & Stassun, K. G. 2007, ApJ, 665, L155
 Messina, S., Lanzafame, A. C., Malo, L., et al. 2017, A&A, 607, A3
 Rebull, L. M., Stauffer, J. R., Cody, A. M., et al. 2018, AJ, 155, 196
 Rebull, L. M., Wolff, S. C., & Strom, S. E. 2004, AJ, 127, 1029
 Ribas, Á., Merín, B., Bouy, H., & Maud, L. T. 2014, A&A, 561, A54
 Scargle, J. D. 1982, ApJ, 263, 835
 Shu, F., Najita, J., Ostriker, E., et al. 1994, ApJ, 429, 781
 Stauffer, J., Rebull, L., Bouvier, J., et al. 2016, AJ, 152, 115
 Stauffer, J., Rebull, L., Cody, A. M., et al. 2018, ArXiv e-prints

Table 1. EPIC ID number of the 49 binaries considered in the present study; color-corrected integrated $(V-K)_0$ color, colors, masses, and rotation periods for the primary and secondary components, respectively; I magnitude of the whole system, and magnitude difference between the two components.

| EPIC ID | $(V-K)_0^{(a)}$ (mag) | $(V-K)_{0P}$ (mag) | $(V-K)_{0S}$ (mag) | $M1^{(b)}$ (M_\odot) | $M2$ (M_\odot) | $P1^{(a)}$ (d) | $P2^{(a)}$ (d) | I mag ^(b) (mag) | $\Delta I^{(b)}$ (mag) | separation ^(b) (AU) |
|----------------|--------------------------|-----------------------|-----------------------|-----------------------------|-----------------------|-------------------|-------------------|-------------------------------|---------------------------|-----------------------------------|
| EPIC 203553934 | 4.65 | 4.61 | 4.69 | 0.59 | 0.55 | 4.70 | 6.22 | 11.47 | 0.20 | 52.57 |
| EPIC 204918279 | 6.23 | 6.12 | 6.38 | 0.29 | 0.25 | 0.46 | 0.47 | 12.60 | 0.20 | 25.57 |
| EPIC 204104740 | 4.83 | 4.81 | 4.85 | 0.56 | 0.54 | 5.57 | 3.06 | 11.55 | 0.10 | 22.41 |
| EPIC 204832936 | 4.98 | 4.87 | 6.20 | 0.38 | 0.03 | 4.26 | 4.98 | 12.86 | 1.80 | 201.46 |
| EPIC 204477741 | 5.86 | 5.86 | 5.86 | 0.31 | 0.31 | 0.82 | 0.76 | 12.74 | 0.00 | 7.39 |
| EPIC 204878974 | 4.22 | 4.14 | 4.33 | 0.56 | 0.48 | 3.09 | 0.85 | 11.16 | 0.40 | 12.68 |
| EPIC 204350593 | 5.13 | 5.10 | 5.17 | 0.42 | 0.40 | 3.16 | 0.98 | 12.16 | 0.10 | 14.87 |
| EPIC 204406748 | 4.52 | 4.43 | 4.64 | 0.69 | 0.57 | 4.39 | 16.96 | 11.14 | 0.60 | 39.78 |
| EPIC 203690414 | 5.33 | 5.15 | 5.65 | 0.32 | 0.24 | 1.82 | 1.95 | 12.95 | 0.40 | 25.57 |
| EPIC 204794876 | 4.02 | 3.94 | 4.13 | 0.73 | 0.61 | 1.49 | 2.15 | 10.87 | 0.60 | 8.71 |
| EPIC 204862109 | 4.15 | 4.12 | 4.18 | 0.73 | 0.69 | 1.73 | 1.05 | 10.88 | 0.20 | 13.64 |
| EPIC 204637622 | 5.06 | 5.06 | 5.06 | 0.50 | 0.50 | 1.05 | 1.39 | 11.99 | 0.00 | 8.84 |
| EPIC 204603210 | 5.19 | 5.00 | 5.59 | 0.39 | 0.27 | 1.09 | 1.22 | 12.42 | 0.60 | 12.35 |
| EPIC 204856827 | 5.15 | 5.15 | 5.15 | 0.44 | 0.44 | 1.65 | 2.81 | 12.13 | 0.00 | 9.56 |
| EPIC 204242152 | 5.08 | 5.08 | 5.08 | 0.45 | 0.45 | 2.10 | 1.57 | 12.33 | 0.00 | 11.06 |
| EPIC 204757338 | 5.75 | 5.75 | 5.75 | 0.30 | 0.30 | 2.30 | 1.06 | 12.94 | 0.00 | 80.98 |
| EPIC 204845955 | 5.22 | 5.13 | 5.34 | 0.53 | 0.45 | 1.20 | 2.53 | 11.66 | 0.40 | 8.86 |
| EPIC 204229583 | 4.89 | 4.71 | 5.32 | 0.55 | 0.35 | 0.69 | 0.77 | 11.54 | 1.00 | 329.27 |
| EPIC 203851147 | 5.33 | 5.13 | 5.75 | 0.38 | 0.26 | 5.91 | 5.34 | 12.37 | 0.60 | 90.92 |
| EPIC 205087483 | 4.98 | 4.98 | 4.98 | 0.46 | 0.46 | 1.51 | 2.38 | 12.23 | 0.00 | 119.34 |
| EPIC 205177770 | 5.65 | 5.40 | 6.35 | 0.30 | 0.18 | 1.14 | 0.93 | 12.91 | 0.60 | 21.31 |
| EPIC 204429883 | 5.74 | 5.74 | 5.74 | 0.38 | 0.38 | 0.32 | 0.33 | 12.20 | 0.00 | 17.05 |
| EPIC 204608292 | 4.50 | 4.35 | 5.97 | 0.36 | 0.10 | 4.40 | 0.83 | 12.38 | 1.30 | 10.91 |
| EPIC 203036995 | 5.33 | 5.11 | 5.87 | 0.38 | 0.24 | 0.93 | 0.78 | 12.39 | 0.70 | 17.05 |
| EPIC 203716047 | 5.14 | 4.95 | 5.54 | 0.39 | 0.27 | 0.85 | 1.44 | 12.43 | 0.60 | 65.35 |
| EPIC 204857023 | 4.44 | 4.31 | 4.64 | 0.54 | 0.42 | 1.46 | 1.86 | 12.46 | 0.60 | 255.36 |
| EPIC 203048597 | 5.33 | 5.33 | 5.33 | 0.39 | 0.39 | 1.61 | 1.17 | 12.31 | 0.00 | 105.13 |
| EPIC 204156820 | 4.57 | 4.57 | 4.57 | 0.59 | 0.59 | 6.61 | 2.62 | 11.74 | 0.00 | 78.14 |
| EPIC 205225696 | 5.19 | 5.19 | 5.19 | 0.34 | 0.34 | 2.70 | 0.89 | 13.26 | 0.00 | 29.83 |
| EPIC 203777800 | 4.95 | 4.91 | 4.99 | 0.39 | 0.37 | 2.28 | 1.25 | 12.65 | 0.10 | 28.41 |
| EPIC 204449800 | 6.25 | 6.25 | 6.25 | 0.31 | 0.31 | 2.45 | 1.95 | 12.58 | 0.00 | 130.05 |
| EPIC 204235325 | 5.11 | 4.88 | 6.19 | 0.44 | 0.20 | 24.03 | 2.01 | 12.11 | 1.20 | 98.19 |
| EPIC 202533810 | 4.78 | 4.78 | 4.78 | 0.52 | 0.52 | 5.04 | 1.73 | 11.80 | 0.00 | 24.15 |
| EPIC 204204606 | 5.31 | 5.31 | 5.31 | 0.33 | 0.33 | 1.15 | 1.49 | 12.86 | 0.00 | 38.36 |
| EPIC 204082531 | 5.81 | 5.81 | 5.81 | 0.27 | 0.27 | 0.65 | 0.43 | 12.78 | 0.00 | 7.59 |
| EPIC 203855509 | 5.41 | 5.25 | 5.68 | 0.35 | 0.27 | 4.52 | 0.39 | 12.93 | 0.40 | 11.03 |
| EPIC 203809317 | 4.55 | 4.44 | 4.72 | 0.52 | 0.42 | 6.46 | 2.39 | 12.36 | 0.50 | 58.25 |
| EPIC 204569229 | 4.22 | 4.16 | 4.30 | 0.66 | 0.58 | 22.92 | 1.26 | 11.27 | 0.40 | 6.63 |
| EPIC 204655550 | 4.20 | 4.06 | 4.47 | 0.63 | 0.45 | 4.03 | 6.08 | 11.41 | 0.90 | 10.28 |
| EPIC 204374147 | 4.59 | 4.47 | 4.80 | 0.71 | 0.53 | 0.62 | 0.49 | 11.05 | 0.90 | 11.48 |
| EPIC 203001867 | 4.78 | 4.71 | 4.86 | 0.53 | 0.47 | 5.32 | 0.83 | 11.91 | 0.30 | 62.51 |
| EPIC 204462113 | 4.60 | 4.53 | 4.69 | 0.40 | 0.36 | 5.73 | 1.07 | 12.69 | 0.20 | 10.12 |
| EPIC 203071614 | 5.72 | 5.52 | 6.11 | 0.29 | 0.21 | 0.46 | 0.53 | 12.55 | 0.40 | 13.65 |
| EPIC 204520585 | 4.25 | 4.13 | 4.46 | 0.70 | 0.52 | 19.16 | 2.16 | 11.75 | 0.90 | 18.65 |
| EPIC 203856244 | 6.08 | 5.94 | 6.31 | 0.44 | 0.34 | 4.07 | 1.95 | 12.11 | 0.50 | 23.49 |
| EPIC 203850605 | 4.85 | 4.85 | 4.85 | 0.60 | 0.60 | 3.92 | 3.52 | 10.76 | 0.00 | 16.86 |
| EPIC 203115615 | 4.73 | 4.58 | 5.02 | 0.65 | 0.45 | 26.17 | 0.99 | 12.36 | 1.00 | 28.58 |
| EPIC 202615424 | 4.30 | 4.30 | 4.30 | 0.52 | 0.52 | 2.82 | 3.69 | 12.34 | 0.00 | 18.47 |
| EPIC 203873374 | 5.23 | 5.20 | 5.26 | 0.48 | 0.46 | 2.06 | 0.63 | 12.50 | 0.10 | 26.99 |

(a): values taken from Rebull et al. 2018; (b): values taken from Tokovinin & Briceño 2018